



Using spatially explicit data to improve our understanding of land supply responses: An application to the cropland effects of global sustainable irrigation in the Americas[☆]

Nelson B. Villoria^{a,*}, Jing Liu^b

^a Department of Agricultural Economics at Kansas State University, United States

^b Department of Agricultural Economics at Purdue University, United States

ARTICLE INFO

Keywords:

Land use
Land supply
Land supply elasticity
Spatially explicit model
Global to local analysis

ABSTRACT

Land supply elasticities determine the rates of land conversion in global policy models. However, they are only available for few countries in the world. Therefore, analysts seeking to improve the spatial resolution of their models are forced to impose regionally homogeneous parameters over highly heterogeneous regions. This article estimates spatially explicit land supply elasticities using gridded data for the American continent. These estimates reasonably reproduce changes in land use observed at different levels of geographical aggregation across the continent. Plugging our estimates in a previous analysis of the land-use effects of eliminating global unsustainable irrigation, reveals higher pressure to convert land in the ecoregions in the south of the continent that have experienced most rapid cropland expansion in the recent past.

1. Introduction

Global economic models are an essential tool in the analysis and design of policies related to the sustainability of global agriculture. For instance, in the U.S., regulation of the ethanol industry is based on model predictions of greenhouse gas emissions from domestic and foreign land use changes caused by biofuel mandates (Babcock, 2009). Beyond biofuels, global trade models have been used to model the land use changes associated with technological change (Villoria et al., 2014), international trade (van Meijl et al., 2006; Verburg et al., 2009), climate change mitigation (Golub et al., 2009), and agricultural policies (Eickhout et al., 2007). Yet, although global models are useful to quantify aggregate outcomes, policy decisions are often made at very localized levels. Recognizing the interdependence between global drivers of land use change and local stressors and policy responses, there is a growing demand to increase the spatial resolution of economic models so that they produce results that are both consistent and accurate at different geographic scales (Verburg et al., 2013).

A crucial obstacle in the development of better models is the paucity of data and parameters characterizing the heterogeneity of economic responses across space. This paucity is particularly acute in many developing and emerging economies, which are precisely the places where

the transformations of the landscape are being most acute. A prime example of this paucity are the land supply elasticities. The land supply elasticity is the percentage change in cropland following a one percent increase in the land rents accruing to agriculture (relative to alternative uses.) These elasticities determine the amount of natural lands that are converted into cropland and, by extension, condition model predictions about environmental metrics linked to land conversion, such as greenhouse gases emissions, biodiversity losses, or changes in the hydrological balance. As economic models increase their spatial resolution, modelers have to grapple with the fact that the available land supply elasticities are either calibrated to match country-level historical patterns of land use changes (Taheripour and Tyner, 2013) or based on econometric evidence which is heavily focused on the U.S. (Lubowski, 2002; Ahmed et al., 2008).

This article contributes to improve the ability of economic models to produce policy insights consistent across geographic scales by estimating spatially heterogeneous land supply elasticities. We focus on the contiguous countries in the Americas, from Canada to Argentina. To preview our main results, we find that the estimated elasticities reasonably reproduce actual changes in cropland observed by Lark et al. (2015) and Graesser et al. (2015) in the US and Latin America. We also find that using these elasticities for policy analysis does indeed provide

[☆] This work has been possible due to generous support from the Energy Policy Research Institute, the Geospatial Building Blocks project (NSF Grant #1261727), and the GEOSHARE project. The authors thank Tyler Lark, Meghan Salmon, and Holly Gibbs for graciously sharing their data on land use change in the U.S. The quality of this article was considerably improved by the generous feedback from two anonymous referees.

* Corresponding author at: Kansas State University, 222 Waters Hall, Manhattan, KS 66506-4011, United States.

E-mail addresses: nvilloria@ksu.edu (N.B. Villoria), liu207@purdue.edu (J. Liu).

more refined insights than current practice. In particular, the use of our elasticities for the analysis of the consequences of eliminating unsustainable irrigation by Liu et al. (2017) suggests increased pressure in the Brazilian Cerrado and other ecoregions of South America already experiencing large pressures for land conversion to agriculture.

The rest of the article is structured as follows. Section 2 discusses the conceptual and empirical underpinnings of a strategy to spatialize the country level supply responses combining the standard theory of land use choice with von Thünen's model of location-determined land rents. Section 3 presents the regression results and discusses the determinants of the estimated land supply elasticities. Section 4 compares prediction of our estimates to actual changes in cropland observed at the level of ecoregions or subnational units. Section 5 demonstrates the use of our estimates by plugging them in the gridded model used by Liu et al. (2017) to explore the consequences of more rational global irrigation practices. Section 6 concludes the article.

2. Modeling framework and empirical strategy

2.1. Theory

We define a land supply schedule as the functional relationship between the quantity of land converted from a natural cover (e.g., forests) to agriculture and the agricultural land rents. To fix ideas, using Z_i and R_i to denote the share of cropland and land rents in each gridcell i , the land supply schedule is given by:

$$Z_i = \epsilon_i^* R_i, \tag{1}$$

where ϵ_i^* is the land supply elasticity in gridcell i . In principle, a regression of Z_i on R_i can be used to get an estimate of ϵ_i^* . However, calculating R_i requires gridcell level input and output prices. Unfortunately, spatially explicit data on either prices or land rents are largely unavailable for most countries of the world.

Following Chomitz and Gray (1996), spatially disaggregated land rents can be approximated using Von Thünen's assumption that spatial differentials in output and input prices are related solely to differences in transport costs to major markets.¹ This allows mapping (up to a proportionality factor) land rents in each gridcell onto market access (A_i) and a vector of k fixed biophysical and socioeconomic covariates ($S_{k[i]}$) that influence land use choices. Formally:

$$R_i \propto f(A_i, S_{k[i]}), \quad k = 1, \dots, K. \tag{2}$$

Substituting (2) in (1) allows expressing the land supply schedules in terms of market access and land suitability, both of which are readily available in the gridded maps described in the Data subsection just below:

$$Z_i = \epsilon_i f(A_i, S_{k[i]}). \tag{3}$$

A caveat to keep in mind is that in this strategy, the resulting elasticity is with respect to market access and not with respect to land rents. Under this modeling framework, these elasticities are proportional to each other, i.e. $\epsilon_i \propto \epsilon_i^*$, but without information on land rents at each gridcell, we are unable to determine the proportionality factor. Nevertheless, to the extent that the spatial heterogeneity of the land supply responses can be reasonably considered to be invariant to scale, the estimated elasticities convey useful information about geographic patterns of supply response. We empirically validate such usefulness below, where the changes in cropland implied by our estimates are compared to observed changes at different levels of geographic aggregation.

Under standard assumptions about producer behavior (in RA S-1),

¹ Formal development of the model and derivation of the regression equation is in Section S-1 of the Reviewers' Appendix to be posted as Supporting On-line Materials upon publication.

Table 1
Descriptive statistics.

	Mean	s.d.	Min	Max
Cropland (share of gridcell, 0–1)	0.12	0.22	0.00	1.00
Market access index (0–1)	0.12	0.21	0.00	1.00
Area equipped for irrigation (% of gridcell)	1.51	6.96	0.00	100.00
Precipitation (mm)	1148.75	788.75	0.00	7513.00
Temperature (°C)	17.06	7.93	−0.78	28.33
Elevation (m)	666.80	801.87	−224.00	5419.00
Soil fertility (IIASA classes)	4.19	2.14	1.00	7.00
Soil carbon density (kg-C/m ²)	5.92	2.45	1.33	24.88
Soil pH (0–14)	6.08	1.00	4.20	8.22
Built-up land (% of gridcell)	0.58	3.94	0.00	100.00
Protected areas (binary variable)	(% of gridcells under each class)			
Unprotected (U)				87
Protected (P)				13
Natural potential vegetation	(% of gridcells under each class)			
Shrublands (S)				13
Tropical forests (Ft)				28
Temperate forests (FT)				28
Savannas & Grasslands (G)				29
Other				3

Notes: These are summary statistics for the sample of 43,311 observations (out of a total of 433,096) used to estimate the elasticities in Fig. 3. The soil fertility constraints categories employed in the regression are: no constraints, slight constraints, moderate, constrained, severe, very severe, and unsuitable for cultivation which were obtained from IIASA/2012. Sources and steps taken to preprocess the data are in Table S-1 of the RA.

Expression (3) can be estimated as a fractional logistic regression model. The estimating equation that we take to data is:

$$Z_i = \Lambda \left[\alpha_0 + \alpha_1 A_i + \sum_k \alpha_k S_{k[i]} \epsilon_i \right], \tag{4}$$

where Λ is the logistic distribution. The elasticity of the changes in cropland to changes in market access for a specific gridcell is given by:

$$\epsilon_i = \frac{\partial \hat{Z}_i}{\partial A_i} \times \frac{A_i}{\hat{Z}_i} = \lambda_i \left[\hat{\alpha}_0 + \hat{\alpha}_1 A_i + \sum_k \hat{\alpha}_k \log(S_{k[i]}) \right] \hat{\alpha}_1 \times \frac{A_i}{\hat{Z}_i}. \tag{5}$$

where λ is the probability distribution function of the logistic distribution and \hat{Z}_i are fitted cropland shares using the parameter estimates ($\hat{\alpha}$) from Eq. (4). Note that the partial effects $\partial \hat{Z}_i / \partial A_i^{-1}$ are specific to each gridcell. This is a property of the logistic model that gives us great flexibility to aggregate the elasticities to different regions or relevant units of spatial analysis.

2.2. Data

Table 1 reports the descriptive statistics of all the variables used to estimate Eq. (4). The dependent variable is the share of each gridcell that was under cropland circa year 2000. This variable was derived by Ramankutty et al. (2008) by combining agricultural inventory data and satellite-derived land cover data.

The market access variable comes directly from Verburg et al. (2011), who combines spatially explicit global data on physical distance, network infrastructure, and underlying terrain to develop a high spatial resolution (1 km²) index of market accessibility determined by the traveling time from each gridcell to the closest and most influential market. The influence of the market is given by market size: Large markets include cities with more than 750,000 inhabitants and maritime ports, while small markets include cities with more than 50,000 inhabitants. The authors assume that large markets are twice as important as smaller markets, and for each grid cell i in the global map, they assign a market influence index (A_i) based on traveling time. The market access index ranges from 0 (inaccessible) to 1 (on a major

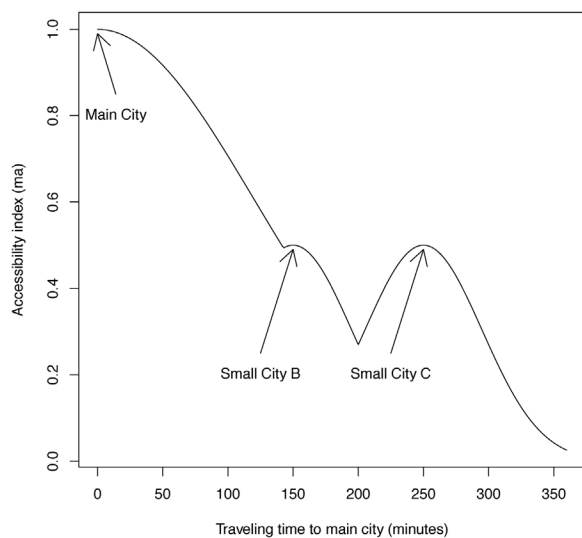


Fig. 1. Market access index decreases (from 1 to 0) as travel time from the Main City increases. Adapted from Verburg, Ellis, and Letourneau (2011, Fig. 2). At 150 and 250 min from the large city are two regional markets.

market), and ranks locations according to traveling time to major cities (Fig. 1).

Potential vegetation is an important variable in our work because it identifies the natural land cover from which there is a transition to cropland. The data on grid cell level potential vegetation are from Ramankutty and Foley (1999). These data are based on satellite imagery and indicate the dominant vegetation type in each grid cell that “would likely exist now in the absence of human activities” for both cultivated and uncultivated grid cells. The original data from Ramankutty and Foley (1999) divides natural potential vegetation into 15 vegetation types, which we further aggregate into five land covers: temperate forests, tropical forests, grasslands, shrublands, and a residual category we label “other” (see Table S-2 in the appendix for the correspondence between Ramankutty and Foley (1999)’s vegetation types and our aggregated categories).

We also add other covariates that aim to capture the role of biophysical and socioeconomic factors in the cropland share. Biophysical factors include: soil fertility constraints (seven categories: no constraints, slight constraints, moderate, constrained, severe, very severe, and unsuitable for cultivation) which were obtained from IIASA/2012; global data on grid cell level soil organic carbon density (kg-C/m^2 to 1 m depth), and soil pH (0–14) coming from the SoilData System, which was developed by the Global Soils Data Task from the International Geosphere-Biosphere Program (IGBP-1998). These data are based on statistical resampling of global soil samples (pedon records) that are consistent with the FAO/UNESCO Soil Digital Map of the World.

The average monthly temperature ($^{\circ}\text{C}$) and average annual total precipitation (millimeters/year) over the period 1961–1990 were constructed using the data from New et al. (1999). These data are commonly used for climate and ecosystem modeling and are obtained by interpolating weather station data using latitude, longitude, and elevation as predictors. The elevation data (meters above sea level) were obtained from TerrainBase, a global model of terrain and bathymetry on a regular 5-min grid documented in NOAA (1995). We also add dummies for agroecological zones (IIASA/2012; Monfreda et al., 2009) which capture changes in the length of the growing seasons across the continent.

The socioeconomic data include area equipped for irrigation (expressed as % of the area of each 5 min grid cell) which comes from Siebert et al. (2010). These data are based on global census-based inventory data on irrigation sources and are from the national and sub-national levels. The built-up land data were obtained from SAGE and

are based on observed built-up area density and nighttime lights, which in turn are used to interpolate urban-area density for those sites in which only nighttime lights are observed. The 5-min resolution data layer identifying the protected areas was obtained from van Velthuisen et al. (2006).

2.3. Methods

Eq. (4) is estimated using the fractional logit estimator of Papke and Wooldridge (1996). To deal with the potential effects of spatial autocorrelation on the error term on inference, we followed a three pronged strategy. First, we used a spatial bootstrap resampling algorithm proposed by Zhu and Morgan (2004) to obtain empirical variance estimators robust to spatial autocorrelation. Second, we included spatial lags of the independent variables (distance-weighted average value of S and A in the neighboring grid cells). Third, we estimated the model in (4) using randomly taken samples of approximately 10% of the data using a sampling scheme that preserves the gridded structure of the original data (Cressie, 1993).

The combination of spatial sampling and inclusion of spatial lags of the explanatory variables have been found an effective way of decreasing the degree of spatial autocorrelation in the model residuals (Robertson et al., 2009). A potential downside of sampling is that it introduces an additional source of uncertainty as parameter estimates are likely to vary across samples. In order to capture such uncertainty, we relied on the recent resampling techniques proposed by Kleiner et al. (2014). These authors demonstrate that estimation of uncertainty parameters such as variances or confidence intervals for datasets that are too large to be handled in standard computers can be achieved by splitting the total sample into subsamples, which are in turn used to obtain bootstrap estimates of the uncertainty measures. These measures are then averaged over the subsamples to obtain improved estimators on uncertainty. The algorithm used to estimate Eq. (4) is explained in section S-3 of the RA.

3. Results and discussion

3.1. Regression results

To aid with the interpretation of the large number of partial effects produced by the logit model, Fig. 2 displays 95% confidence intervals for these effects averaged across all the gridcells in the estimating sample (parameter estimates and details on the calculations of the APE are in RA S-4). Starting with market access, we find that more accessible gridcells are associated with larger shares of cropland. The estimated confidence interval for the average partial effect implies that an increment in the market access index from, say, 0.7 to 0.8, would translate into an increase in cropland cover of 0.396–0.527 percent. This suggests that although statistically significant, *on average*, market access have a rather small effect on cropland shares. In reality, the distribution of the partial effects of market access across the continent is highly unequal, ranging from nil to about 1.2% (i.e., a 1/10 increment in the market access index leads to a 1.2% increase in cropland shares.)

The area equipped for irrigation in each gridcell also has a positive, statistically different from zero, but albeit small effect on cropland shares; the APE indicates that a unit increase in the area equipped for irrigation drives up the share of cropland by 0.24–0.28 percentage points. The estimated effects of precipitation and elevation on cropland shares are practically indistinguishable from zero. But the effect of temperature is somehow larger, with a positive linear term and a negative quadratic term. The average partial effects for the range of temperatures observed in the data is shown in the lower panel of Fig. 2. For very low temperatures (in the neighborhood of zero $^{\circ}\text{C}$), increases in heat during the growing season increase the share of cropland by around 5 percent points (95% CI: 4.8–5.8). This partial effect decreases with higher temperatures, and at approximately 18 $^{\circ}\text{C}$ degree Celsius,

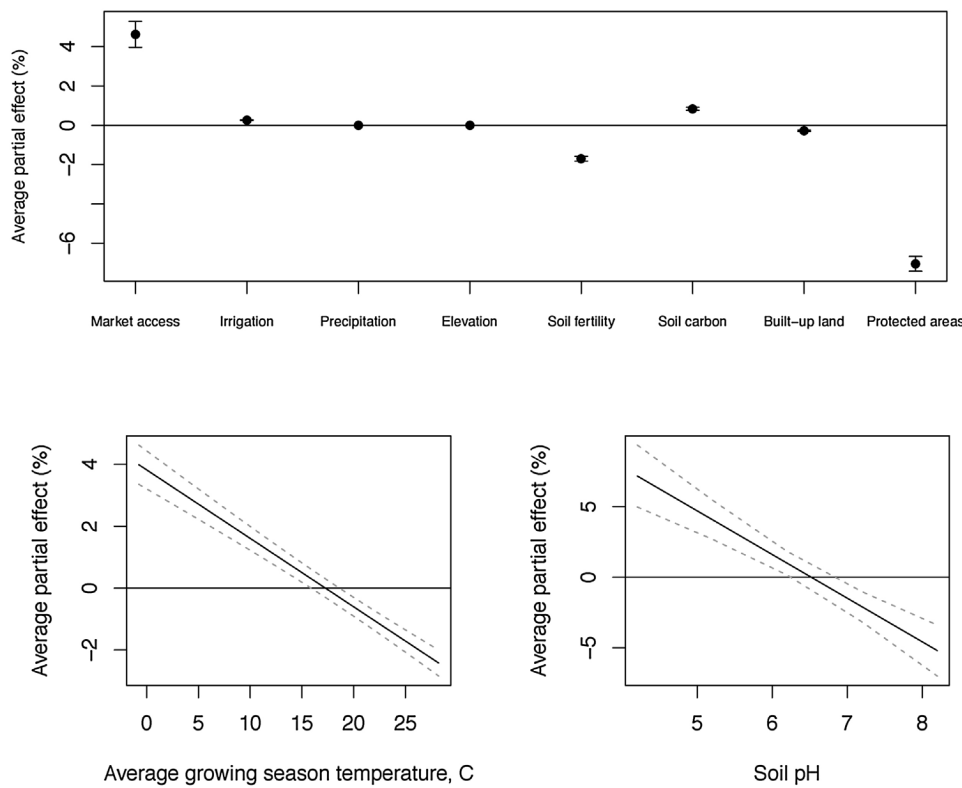


Fig. 2. Point estimates and 95% confidence intervals of average partial effects (APE). The y-axis indicates percentage points increase in cropland shares. APE for variables with quadratic terms (temperature and soil pH) are shown for the in-sample range of each variable. The scale factor of the displayed partial effects were obtained by averaging the logit probability density functions evaluated at each gridcell across all the gridcells in the sample (see Table S-3 in the RA for algebraic expressions of the APE). Standard errors were calculated using the Delta method (Greene, 2008).

higher temperatures reduce the amount of cropland on the average gridcell.

Soil fertility constraints are also significant determinants of the share of land under cropland. Gridcells with less fertile soils are associated with less cropland as a unit increase in the soil fertility scale reduces the cropland share by a 95% CI with bounds -1.8 and -1.6 percent points. Similarly, a unitary increase in soil carbon increases the share of cropland by 0.8 – 0.9 (95% CI) percentage points. The acidity of the soil (pH) has a positive linear effect as well as a quadratic negative effects, and the APE in the lower panel of Fig. 2 suggests that the marginal effect is highest just below neutrality (pH = 7) and declines as the soils become more basic. This finding is in line with the agronomic and global ecology literature, which indicates optimal growing conditions in soils with a pH between 6.6 and 7.0 (Ramankutty et al., 2002).

After correcting for accessibility, a greater share of built-up land is associated with a lower cropland share (a 1% increase in built-up land decreases the share of cropland by around 0.3% with a 95% CI: -0.32 , -0.25), which probably reflects the fact that urban uses are more profitable. We also find that protected areas tend to have lower shares of cropland, around 7% as indicated by a 95% CI with bounds -7.42 and 6.67 , a finding consistent with those of Blankespoor et al. (2017), who find that protected areas are associated with reduced deforestation.

3.2. Land supply elasticities: market access vs. land suitability

Using the parameter estimates just discussed, we use expression (5) to calculate estimates of the elasticity of cropland shares to changes in market access for each one of the approximately 43,300 gridcells in each of the 25 samples and their respective bootstrap samples (Fig. 3a). In this section we explore the determinants of these elasticities as well as their ability to reproduce historical patterns of land use change in the region.

The variation of the land supply elasticities across gridcells is entirely explained by the logit scale factors, $\lambda_i [\alpha_0 + \alpha_1 A_i + \alpha_2 \log(S_i)]$ in Eq. (5), which in turn depend on market access and cropland suitability.

The issue we explore next is the relative importance of these two sources of variation in determining the elasticity of land supply. For this, we recomputed the scale factors by setting the market access index equal to zero (i.e., for each gridcell we computed $\lambda_i [\alpha_0 + \alpha_2 \log(S_i)]$). These recomputed scale factors capture how much of the partial effect of market access is due to land suitability for agriculture while abstracting from the effects of market access.

The scale factors with and without market access as well as their ratio are shown in Fig. 3b, c and d. Notice that for the vast majority of the continent the ratios in Fig. 3d range from 0.6 to 1, indicating that for these gridcells, land suitability drives from 60% to 100% of the land supply response to a change in market access. The implication of this is that in two gridcells with identical market access, the same change in market access will cause a larger amount of land expansion in the gridcell more suitable for agriculture. As a corollary, to the extent that an increase in land profitability can be thought of as an improvement in market access, as proposed by Eq. (2), then, keeping other things equal, gridcells with low suitability would need a higher overall increase in profitability in order to justify their incorporation into production.

4. Validation of regional patterns of land supply response

Two recent studies, Lark et al. (2015) in the US, and Graesser et al. (2015) in Latin America, offer enough spatial detail for validating the spatial patterns of land supply responses discussed above. Graesser et al. (2015) report that from 2001 to 2013, cropland expanded by 44 million hectares (Mha) in Latin America. Approximately 75% of this expansion occurred in ecoregions in the southern part of the continent: the Cerrado in Brazil (≈ 10 Mha), the Humid Pampas in Argentina (≈ 6 Mha), the Alto Paraná Atlantic forest that extends from southern Brazil to eastern Paraguay and northern Argentina (≈ 5 Mha), the Dry Chaco in eastern Bolivia, northern Argentina, part of Brazil, and western Paraguay (≈ 2 Mha); the Uruguayan Savanna (≈ 2 Mha); and the Araucarian moist forests in southern Brazil and Northern Argentina (≈ 2 Mha). Graesser et al. (2015) also report significant expansion of cropland in Mexico (≈ 8 Mha), and in the Llanos, shared by Colombia

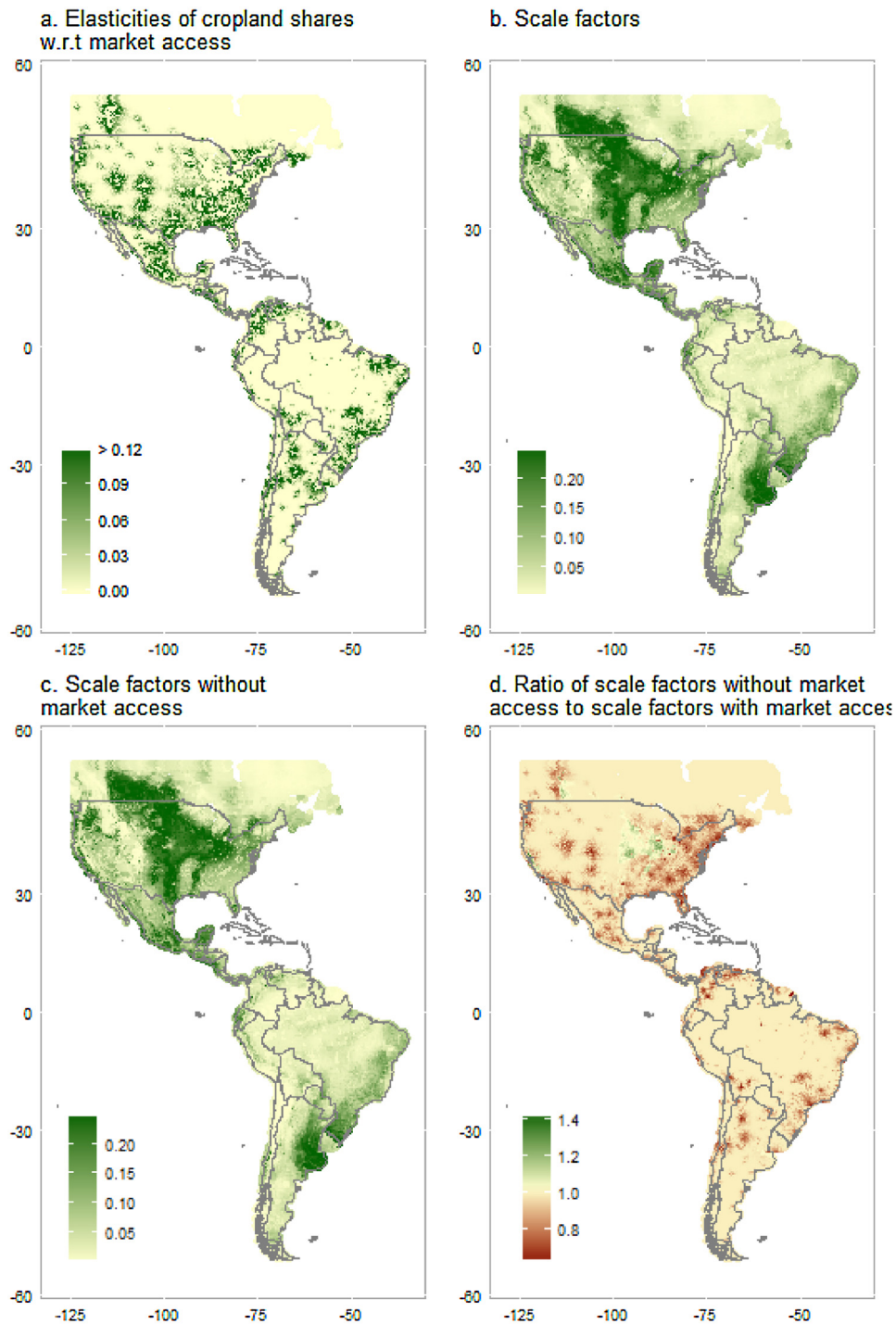


Fig. 3. Land supply responses: market access vs. land suitability. Scale factors are the probability density function of the logistic model (see expression (5)) evaluated at each grid cell.

and Venezuela (≈ 0.4 Mha). The question we ask is to what extent the estimated elasticities predict changes such as these, at the level of ecoregions.

As explained above, the estimated land supply elasticities to market access are conceptually proportional to elasticities to land rents, but given the lack of data on gridded land rents, the exact proportionality is unknown. As a simplifying alternative we assume a proportionality factor that is common to all the countries in which there was significant changes in cropland. This proportionality factor equals 0.9, and is the value of a back-of-the-envelope regional land supply elasticity calculated using FAOSTAT data on cropland and implied land rents (see RA

S-5 for calibration of these elasticities). The scaling up of the elasticities is a linear transformation that preserves the spatial distribution of the original estimates. The changes in cropland during 2001–2013 are obtained by multiplying the scaled elasticities by 19%, which is the cumulative growth in regional changes in implicit land rents from 1999 to 2011, obtained from FAOSTAT (see RA S-5).

As displayed in Fig. 4, the estimated elasticities produce a pattern of land conversion at the level of ecoregions that—with the exception of the Araucaria and Mato Grosso forests—is consistent with the changes observed by Graesser et al. (2015). The Spearman ranking correlation between our estimates and Graesser et al. (2015)'s observations is 0.53

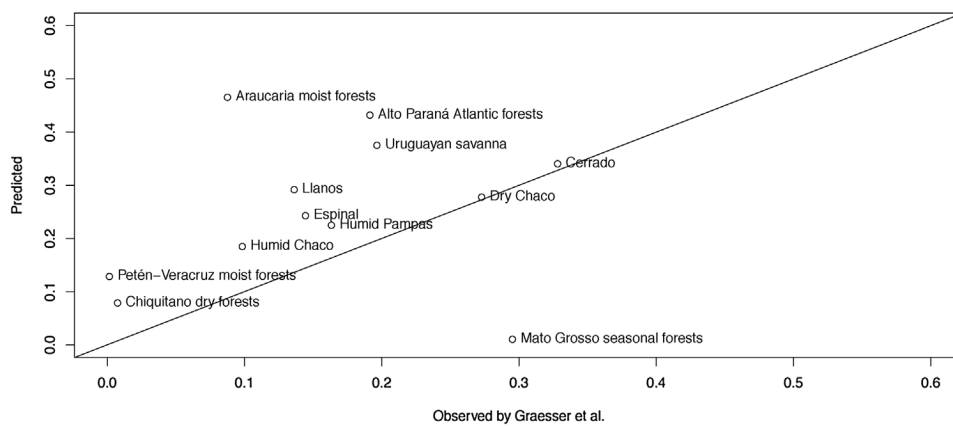


Fig. 4. Predicted vs. observed increases in cropland (relative to cropland in 2000) by ecoregion in Latin America. Observed changes are the number of hectares converted to cropland from non cropland from 2001 to 2013 as reported by Graesser et al. (2015, Fig. S4), divided by the cropland hectares circa 2000 from Ramankutty et al. (2008).

($p < 0.05$) and the Pearson correlation coefficient is 0.52 ($p < 0.05$). When the Araucaria and Mato Grosso forests are excluded, these correlations climb up to 0.77 ($p < 0.05$) and 0.76 ($p < 0.05$). These correlations are invariant to the size of the elasticity used to elicit the changes in land use; their size suggest that land suitability and accessibility go a long way in explaining actual changes in land use in Latin America.

This comparison is purposely focused on eliciting the geographic pattern of land use conversion, not the changes in physical area. This focus obeys to the fact that we rely on few determinants of land use at a fixed point in time. Drivers such as road construction and voluntary commitments to avoid sourcing from deforestation hotspots, among many others, likely overwhelm the role of land suitability and exacerbate the effects of market access on determining the land supply elasticities (Soares-Filho et al., 2004; Noojipady et al., 2017) as well as land returns within these regions. Using region-specific scalars and changes in land rents would probably help to match the observed changes in terms of physical area; however, this would confound the size of the effects with their location. As a consequence, using a single regional land elasticity coupled with a regionally uniform change in land rents is an effective way to discern the geographic pattern of land supply responses, but inadequate to get accurate predictions of the actual changes.

We undertake a similar evaluation of our elasticities for the U.S. In this case, we compare the geographic pattern of land supply response predicted by our elasticities with the gross changes in cropland reported by Lark et al. (2015) in their study of cropland changes during 2008–2012. In this case, their Lark et al. (2015) is available to us at the gridcell level. We focus only on the gridcells with positive net conversion. This allows comparing the accuracy of our estimates in reproducing patterns of land supply response at different scales of interest. We follow a similar procedure as above. First, scale up the elasticities so the average elasticity for the US is 0.03, which is the land supply elasticity estimated by Barr et al. (2011, Table 3) for the same period. The scaled elasticities are then multiplied by an increase in land rents of 0.58 taken also from Barr et al. (2011, Table 3).

We then aggregate the changes in cropland to different subnational and ecological aggregates. Table 2 shows the results. The Spearman rank correlation coefficient for the whole US is 0.58 ($p < 0.01$). When we aggregate at the state level (48 states), we observe a similar rank correlation (0.58, $p < 0.01$) indicating that the estimated elasticities rank states similarly to the ranking reported by Lark et al. (2015). At the even more granular level of counties (3077 units), the rank correlation is still statistically significant and positive (0.42, $p < 0.01$). At the level of ecoregions (71 units), the rank correlation is 0.87 ($p < 0.01$); the increase in accuracy at the ecoregion level is likely associated with the fact that ecoregions encompass relatively homogeneous areas in terms of land suitability for agriculture, and therefore naturally match the variables used to identify the geographic patterns

Table 2

Spearman (rank) and Pearson Correlation coefficients between predicted and observed changes in land use at different level of geographic aggregation in the U.S.

Level	Units	Spearman	Pearson
Country	1	0.58	0.17
Country (NH) ^a	1	0.60	0.23
State	48	0.58	0.47
State ^a	40	0.62	0.69
County	3077	0.42	0.23
County ^a	2360	0.53	0.34
Ecoregion	71	0.87	0.57
Ecoregion ^a	70	0.87	0.55

Notes: Gross cropland expansion in gridcells with positive net change from Lark et al. (2015).

^a Excludes Iowa, Nebraska, Minnesota, Illinois, South Dakota, Kansas, Indiana, and Wisconsin, where 75% of US ethanol refineries are located (ORNL, 2014).

of land supply response.

While the Spearman correlations measure the degree of coincidence in ranking, the Pearson correlations measure the correlation between the magnitude of the changes. For the US as a whole as well as for the 3077 counties, the magnitudes of cropland conversion predicted by the estimated elasticities are uncorrelated with the changes reported by Lark et al. (2015). This indicates that at the level of administrative units, our estimates are reasonable predictors of where cropland expansion takes place but not of how much cropland is supplied from natural lands. However, at the level of ecoregions the Pearson correlation coefficient is 0.57 ($p < 0.01$) strengthening the argument above about the natural congruency between ecoregions and our estimates.

As in the case of Latin America, it is important to keep in mind that these estimates assume a uniform increase in land rents across the vast geography of the U.S., an assumption that may be at odds with the fact that the US displays many different types of agriculture. Moreover, there are well documented processes that are not included in our framework and that have large effects on land use decisions such as farm income and resource conservation policies (Lubowski et al., 2008; Barr et al., 2011). Finally, a main driver of land expansion in the US during this period was the location of ethanol refineries (Wright et al., 2017). Most of the ethanol refineries are concentrated in few states in the mid-west and central plains.² As shown in Table 2, when these states are excluded from the sample, both the Spearman and Pearson correlations increase at every level of administrative unit (country, states and counties), in some cases substantially so. This suggests that future

² According to the ORNL (2014), by 2014, 75% of ethanol refineries were in Iowa, Nebraska, Minnesota, Illinois, South Dakota, Kansas, Indiana, and Wisconsin.

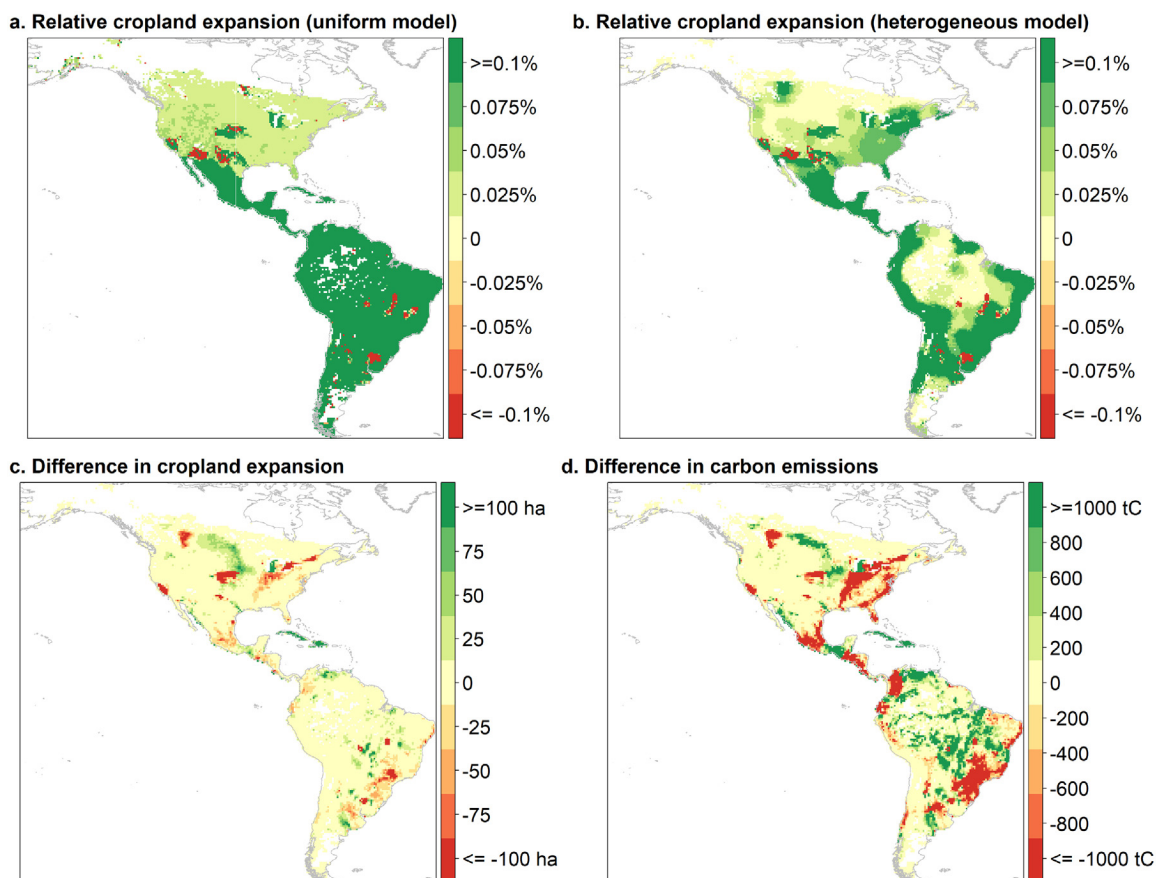


Fig. 5. Relative change in cropland area under two cases: uniform land supply elasticity (top) and spatially heterogeneous elasticity (bottom). Compare absolute change of cropland conversion (top) caused by eliminating unsustainable irrigation and the associated difference in carbon emissions (bottom). The difference is relative to results generated by the model with heterogeneous parameter. Green color indicates the model with uniform parameters may overestimate net cropland conversion or carbon emissions, while red color indicates the opposite. (For interpretation of the references to color in this figure legend, the reader is referred to the web version of this article.)

refinements of this work will benefit from including data on the location of biofuel refineries and other processing plants in the market access measures. Meanwhile, readily available indicators of land use choice and suitability can be used to improve the representation of land supply responses at several scales below the country level.

5. Revisiting the land use impacts of restricting unsustainable irrigation in the Americas

Researchers and policy analysts from many disciplines are increasingly interested in modeling frameworks that reconcile the fact that macro-level policies are often felt very differently at the local level due to the large variation in physical, biophysical, and socio-economic characteristics across space (Verburg et al., 2013). Ignoring the spatial heterogeneity of policy effects can result in misleading findings, rendering the simulation of policies of little use to decision making (Dinar, 2014; Liu et al., 2016).

In this section we explore the additional insights that the estimated site-specific elasticities could provide when incorporated in the evolving economic models that seek to reconcile the effects of global drivers and local policies across different spatial scales by revisiting a study in the frontier of this literature. We do this by revisiting the work of Liu et al. (2017) who analyse the land use and food security effects of pursuing globally sustainable irrigation.

The work of Liu et al. (2017) is an example of the frontier of global economic models for policy analysis. Three features of this work are particularly interesting to us. First, Liu et al. (2017) employ a publicly

available,³ grid-resolving model nicknamed SIMPLE-G—a multi-region, partial equilibrium model of gridded cropland use at a resolution of 30 min with crop production, consumption and trade determined at the level of regions (e.g., Latin America)—, that readily accommodates the resolution of our estimated elasticities. Second, in SIMPLE-G, the potential for cropland to expand is a key factor determining the outcomes of restricting irrigation. The more elastic is the supply of cropland, the larger the possibility expanding land area to compensate production losses from restricting intensification through the rationalization of irrigation. Finally, while the core of SIMPLE-G is spatially explicit, most of the behavioral parameters, including the land supply elasticity, are calibrated at the regional level due to lack of information at a finer scale. Replacing regional parameters with grid-specific ones provides an opportunity to learn the value of improving spatial heterogeneity of the model.

Liu et al. (2017) consider irrigation to be unsustainable if water withdrawals exceed 20% of total annual water available for irrigation. The authors run a suite of experiments that trace the changes in global rain fed and irrigated cropland once that regions with unsustainable irrigation are forced to use no more than 20% of their total water available for irrigation. We focus in their experiment *a* (Liu et al., 2017, Table 1) in which the total factor productivities of irrigated and non-

³ <https://mygeohub.org/resources/simpleg>. Other models with gridcell resolution exist, e.g., MagPIE (Lotze-Campen et al., 2008) and GLOBIOM (Valin et al., 2013), but are not publicly available for this type of exercise.

Table 3

Land conversion in the Americas (in 1000 ha) caused by eliminating global unsustainable irrigation with homogeneous and spatially heterogeneous land supply elasticities.

Region	Homogeneous	Heterogeneous	Difference
Brazil	100.44	120.83	–20.39
Canada	15.27	26.08	–10.81
USA	196.68	269.69	–73.01
Rest of the Americas	185.65	176.06	9.59
Americas total	498.04	592.66	–94.63

Table 4

Carbon emissions in the Americas (in million metric tons of carbon) caused by eliminating global unsustainable irrigation with homogeneous and spatially heterogeneous land supply elasticities.

Region	Homogeneous	Heterogeneous	Difference
Brazil	14.07	15.24	–1.18
Canada	0.55	1.48	–0.92
USA	8.63	9.64	–1.01
Rest of Americas	17.15	15.52	1.63
Americas total	40.40	41.88	–1.48

irrigated crop sectors are assumed to grow in tandem till 2050 without structural market adaptations (business as usual scenario). The authors find that the pursuit of sustainable use of water limits the yield boosting effect of irrigation, and therefore, results in cropland expansion into both rain-fed areas and irrigated area with no stress of water scarcity. Globally, the induced land conversion leads to 0.871 GtC of carbon emissions, which amounts to 9% of global carbon emissions in 2014.

In the present extension, we rerun the same experiment, except that land supply elasticity is updated to vary by grid-cell. Fig. 5 presents the relative change of cropland area under two compared cases uniform and heterogeneous land supply elasticities. In contrast to the fairly homogeneous change in the former, the land conversion in the latter is mostly concentrated in the east of the US, the west coast of the Andean states, and the Cerrado in Brazil. In terms of absolute values (Fig. 5c), the uniform parameter model may over-predict land conversion in the Corn Belt and the Caribbean, but under-predict land conversion on the fringe of Corn Belt, the central plains of Canada, and the southern Cerrado (Brazil-Argentina) and the Argentinian Pampas.

Using gridded carbon stock data (in C/ha) from West et al. (2010), we translate the area of conversion to net carbon emissions in Fig. 5d. The model with uniform regional land supply elasticities tends to overestimate carbon emissions in many parts of the Amazon and the Corn Belt, but underestimate those in the east of the US and the Highland plateau in Brazil. At the regional level, the model updated with the spatially heterogeneous supply responses predicts 95,000 hectares more (about 20% more) of land conversion than the original model, as a result of restricting unsustainable irrigation. Tables 3 and 4 show that the discrepancy mainly arises from Brazil, Canada and the US. However, the associated carbon emissions predicted by the two models are quite similar. In other words, although the updated model predicts more cropland conversion, the expansion is not taking place in locations where carbon stock is high as suggested by the other model.

This comparison demonstrates the additional richness in the outcomes of irrigation conservation that is overlooked if the spatial nuances in agricultural extensification are ignored. Liu et al. (2017) demonstrate the potential trade-offs between different sustainable development goals: the pursuit of sustainable irrigation may erode other development and environmental goals by raising food prices and increasing greenhouse gas emissions. A key contribution of their work is to link localized decisions of water management to global outcomes. Our revision of their work suggests that a refined spatial representation of production behavior regarding land conversion allows for sharper

conclusions about where changes are more likely to occur. In the specific case discussed above, rationalizing worldwide irrigation is likely to exert even more pressure in ecosystems in the southern part of the continent that are already experiencing high rates of land conversion discussed in the previous section. Being able to better understand the interactions between better global water management and localized land conversion should improve the process of both local and global policy formulation.

6. Conclusions

Recognizing the interdependence of global and local changes there is a growing demand to increase the spatial resolution of economic models. A key limitation for these models is the lack on data and parameters at disaggregated levels. We contribute to these models by estimating a key parameter, namely, the land supply elasticities. Due to data limitations, the identification of these elasticities comes from cross-sectional variation in cropland shares, market access, and land suitability across the American continent. Unavoidably, this leaves out many key determinants of land use change such as changes in policy objectives associated with economic development and environmental protection, land governance, and other factors. Nevertheless, land use predictions of our estimates aggregated to either subnational administrative or ecological regions, compare favorably to observed recent changes in land use in the US and Latin America by Lark et al. (2015) and Graesser et al. (2015). This suggests that the proposed framework and estimates can be used to spatialize land supply elasticities observed at the national level, increasing the accuracy of spatially explicit economic models. We offer an example of this by embedding our estimates into a gridded model of the global economy used to explore the consequences of eliminating worldwide unsustainable irrigation practices. Our results demonstrate that although the aggregated outcomes are relatively insensitive to increased spatial resolution, the model with heterogeneous parameters indicates that the brunt of the land expansion from less wasteful global irrigation practices is precisely in the Brazilian Cerrado and Argentinian Pampas, places that have been under great pressure for cropland expansion during the last decade.

Appendix A. Supplementary data

Supplementary data associated with this article can be found, in the online version, at <https://doi.org/10.1016/j.landusepol.2018.04.010>.

References

- Ahmed, S., Hertel, T.W., Lubowski, R., 2008. Calibration of a Land Cover Supply Function Using Transition Probabilities. GTAP Research Memorandum No. 14. GTAP Center, Department of Agricultural Economics, Purdue University.
- Babcock, B., 2009. Measuring Unmeasurable Land-Use Changes from Biofuels. Iowa Ag Review No. 15. Iowa State University, Iowa.
- Barr, K.J., Babcock, B.A., Carriquiry, M.A., Nassar, A.M., Harfuch, L., 2011. Agricultural land elasticities in the United States and Brazil. *Appl. Econ. Perspect. Policy* 33, 449–462.
- Blankespoor, B., Dasgupta, S., Wheeler, D., 2017. Protected areas and deforestation: new results from high-resolution panel data. *Nat. Resour. Forum* 41, 55–68.
- Chomitz, K.M., Gray, D.A., 1996. Roads, land use, and deforestation: a spatial model applied to Belize. *World Bank Econ. Rev.* 10, 487–512.
- Cressie, N., 1993. *Statistics for Spatial Data*. John Wiley & Sons, New York, Chichester, Toronto, Brisbane, Singapore.
- Dinar, A., 2014. Water and economy-wide policy interventions. *Found. Trends[®] Microecon.* 10, 85–165.
- Eickhout, B., van Meijl, H., Tabeau, A., van Rheenen, T., 2007. Economic and ecological consequences of four European land use scenarios. *Land Use Policy* 24, 562–575.
- Golub, A., Hertel, T., Lee, H.L., Rose, S., Sohngen, B., 2009. The opportunity cost of land use and the global potential for greenhouse gas mitigation in agriculture and forestry. *Resour. Energy Econ.* 31, 299–319.
- Graesser, J., Aide, T.M., Grau, H.R., Ramankutty, N., 2015. Cropland/pastureland dynamics and the slowdown of deforestation in Latin America. *Environ. Res. Lett.* 10, 034017.
- Greene, W.H., 2008. *Econometric Analysis*, 6th ed. Prentice Hall, Upper Saddle River NJ.
- IGBP-DIS, 1998. *SoilData(V.0) A Program for Creating Global Soil-Property Databases*, IGBP Global Soils Data Task, France.

- IIASA/FAO, 2012. Global Agro-Ecological Zones (GAEZ v3.0). IIASA, Laxenburg, Austria and FAO, Rome, Italy.
- Kleiner, A., Talwalkar, A., Sarkar, P., Jordan, M.I., 2014. A scalable bootstrap for massive data. *J. R. Stat. Soc.: Ser. B (Stat. Methodol.)* 76, 795–816.
- Lark, T.J., Salmon, J.M., Gibbs, H.K., 2015. Cropland expansion outpaces agricultural and biofuel policies in the United States. *Environ. Res. Lett.* 10, 044003.
- Liu, J., Hertel, T., Taheripour, F., 2016. Analyzing future water scarcity in computable general equilibrium models. *Water Econ. Policy* 02, 1650006.
- Liu, J., Hertel, T.W., Lammers, R.B., Prusevich, A., Baldos, U.L.C., Grogan, D.S., Frolick, S., 2017. Achieving sustainable irrigation water withdrawals: global impacts on food security and land use. *Environ. Res. Lett.* 12, 104009.
- Lotze-Campen, H., Müller, C., Bondeau, A., Rost, S., Popp, A., Lucht, W., 2008. Global food demand, productivity growth, and the scarcity of land and water resources: a spatially explicit mathematical programming approach. *Agric. Econ.* 39, 325–338.
- Lubowski, R., 2002. Determinants of Land-Use Transitions in the United States: Econometric Analysis of Changes among the Major Land-Use Categories. Harvard University (PhD Dissertation).
- Lubowski, R., Plantinga, A., Stavins, R., 2008. What drives land-use change in the United States? A national analysis of landowner decisions. *Land Econ.* 84, 529.
- Monfreda, C., Ramankutty, N., Hertel, T., 2009. Global agricultural land use data for climate change analysis. In: Hertel, T.W., Rose, S.K., Tol, R.S. (Eds.), *Economic Analysis of Land Use in Global Climate Change Policy*. Routledge, London/New York, pp. 33–49.
- New, M., Hulme, M., Jones, P., 1999. Representing twentieth-century space-time climate variability. Part I: Development of a 1961–90 mean monthly terrestrial climatology. *J. Climate* 12, 829–856.
- NOAA, 1995. TerrainBase, Global 5 Arc-Minute Ocean Depth and Land Elevation from the US National Geophysical Data Center (NGDC).
- Noojipady, P., Morton, C.D., Macedo, N.M., Victoria, C.D., Huang, C., Gibbs, K.H., Bolfe, L.E., 2017. Forest carbon emissions from cropland expansion in the Brazilian Cerrado Biome. *Environ. Res. Lett.* 12, 025004.
- ORNL, 2014. Oak Ridge National Laboratory National Refineries Database, <https://openei.org/datasets/dataset/national-biorefineries-database>.
- Papke, L.E., Wooldridge, J.M., 1996. Econometric methods for fractional response variables with an application to 401(k) plan participation rates. *J. Appl. Econom.* 11, 619–632.
- Ramankutty, N., Evan, A.T., Monfreda, C., Foley, J.A., 2008. Farming the planet: 1. Geographic distribution of global agricultural lands in the year 2000. *Glob. Biogeochem. Cycles* 22.
- Ramankutty, N., Foley, J.A., 1999. Estimating historical changes in global land cover: croplands from 1700 to 1992. *Glob. Biogeochem. Cycles* 13, 997–1027.
- Ramankutty, N., Foley, J.A., Norman, J., McSweeney, K., 2002. The global distribution of cultivable lands: current patterns and sensitivity to possible climate change. *Glob. Ecol. Biogeogr.* 11, 377–392.
- Robertson, R.D., Nelson, G.C., De Pinto, A., 2009. Investigating the predictive capabilities of discrete choice models in the presence of spatial effects. *Pap. Reg. Sci.* 88, 367–388.
- Siebert, S., Burke, J., Faures, J.M., Frenken, K., Hoogeveen, J., Döll, P., Portmann, F.T., 2010. Groundwater use for irrigation – a global inventory. *Hydrol. Earth Syst. Sci.* 14, 1863–1880.
- Soares-Filho, B., Alencar, A., Nepstad, D., Cerqueira, G.M., Vera Diaz, d.C., Rivero, S., Solórzano, L., Voll, E., 2004. Simulating the response of land-cover changes to road paving and governance along a major Amazon highway: the Santarém-Cuiabá corridor. *Glob. Change Biol.* 10, 745–764.
- Taheripour, F., Tynner, W., 2013. Biofuels and land use change: applying recent evidence to model estimates. *Appl. Sci.* 3, 14–38.
- Valin, H., Havlík, P., Mosnier, A., Herrero, M., Schmid, E., Obersteiner, M., 2013. Agricultural productivity and greenhouse gas emissions: trade-offs or synergies between mitigation and food security? *Environ. Res. Lett.* 8, 035019.
- van Meijl, H., van Rheenen, T., Tabeau, A., Eickhout, B., 2006. The impact of different policy environments on agricultural land use in Europe. *Agric. Ecosyst. Environ.* 114, 21–38.
- van Velthuisen, H., Huddleston, B., Fischer, G., Salvatore, M., Ataman, E., Nachtergaele, F., Zanetti, M., Bloise, M., 2006. Mapping Biophysical Factors That Influence Agricultural Production and Rural Vulnerability. Working paper No. 11, Food and Agriculture Organisation of the United Nations & IIASA.
- Verburg, P.H., Ellis, E.C., Letourneau, A., 2011. A global assessment of market accessibility and market influence for global environmental change studies. *Environ. Res. Lett.* 6, 034019.
- Verburg, P.H., Erb, K.H., Mertz, O., Espindola, G., 2013. Land system science: between global challenges and local realities. *Curr. Opin. Environ. Sustain.* 5, 433–437.
- Verburg, R., Stehfest, E., Woltjer, G., Eickhout, B., 2009. The effect of agricultural trade liberalisation on land-use related greenhouse gas emissions. *Glob. Environ. Change* 19, 434–446.
- Villoria, N.B., Byerlee, D., Stevenson, J., 2014. The effects of agricultural technological progress on deforestation: what do we really know? *Appl. Econ. Perspect. Policy* 36, 211–237.
- West, P.C., Gibbs, H.K., Monfreda, C., Wagner, J., Barford, C.C., Carpenter, S.R., Foley, J.A., 2010. Trading carbon for food: global comparison of carbon stocks vs. crop yields on agricultural land. *Proc. Natl. Acad. Sci. U. S. A.* 107, 19645–19648.
- Wright, C.K., Larson, B., Lark, T.J., Gibbs, H.K., 2017. Recent grassland losses are concentrated around U.S. ethanol refineries. *Environ. Res. Lett.* 12, 044001.
- Zhu, J., Morgan, G.D., 2004. Comparison of spatial variables over subregions using a block bootstrap. *J. Agric. Biol. Environ. Stat.* 9, 91–104.